Available online at www.sciencedirect.com
ScienceDirect
Journal of Power Sources 165 (2007) 359–367
JOURNAL OF POWER SOURCES
www.elsevier.com/locate/jpowsour

# Effect of oxygen non-stoichiometry and temperature on cation ordering in $LiMn_{2-x}Ni_xO_4$ ($0.50 \geq x \geq 0.36$) spinels

Muharrem Kunduraci *, Glenn G. Amatucci

*Energy Storage Research Group, Department of Materials Science and Engineering, Rutgers, The State University of New Jersey, North Brunswick, NJ 08902, USA*

Received 1 November 2006; received in revised form 22 November 2006; accepted 23 November 2006
Available online 5 January 2007

**Abstract**

The effect of oxygen stoichiometry on the transition metal ordering and electrochemical activity of $LiMn_{2-x}Ni_xO_4$ solid solutions was investigated. Temperature–oxygen-partial-pressure–composition ($pO_2$–$T$–$x$) diagrams of ordered and disordered phases of $LiMn_{2-x}Ni_xO_4$ ($0.50 \geq x \geq 0.36$) in the vicinity of order–disorder transition temperature ($T_c$) was constructed by means of infrared spectroscopy, thermogravimetric analysis and galvanostatic measurements. Despite their simplicity and limitations over traditional diffraction techniques, all three techniques offered near excellent capability to distinguish ordered and disordered phases. The effect of oxygen-partial-pressure ($pO_2$) in the annealing atmosphere and nickel content of the spinel on $T_c$ was studied. The transition temperature increased with $pO_2$ and nickel content, except in oxygen-rich ($pO_2 = 1$) atmosphere for the maximum nickel content spinel of $LiMn_{1.5}Ni_{0.5}O_4$. An explanation for the dependence of the transition temperature on the two variables and changes induced by the post-fabrication heat treatments is provided.


*Keywords:* Lithium-ion battery; Spinel; Cation ordering; Rate capability; Oxygen-partial-pressure

## 1. Introduction

Lithium secondary batteries are the state-of-the-art power sources for hybrid cars, laptop computers, power tools and many other consumer electronics. Today, about 15 years after its first commercialization, $LiCoO_2$ still dominates the market for positive electrode materials. However, due to the high cost of cobalt metal, research efforts in the last decade have been shifted towards finding intercalation compounds with lower cost transition metals without sacrificing electrochemical performance. The most promising of them are olivine-type $LiFePO_4$ and spinel $LiMn_{2-x}M_xO_4$ (M = transition metal or Li, Al, etc.). While the former chemistry was demonstrated to have high reversible capacity and intrinsic safety thanks to its electrochemically stable phosphate group [1–3], the latter is more of choice in high power applications due to its much higher average discharge potential especially when doped with transition metals [4–7].

Transition metal oxide spinels possess rich crystal chemistries due to the ability of transition metals to adapt different valence states. This can be induced by changing the starting composition, annealing temperature or atmosphere, *i.e.* oxidizing or reducing. Recently, we have reported on the correlation between transition metal ordering, electronic conductivity and electrochemical activity of $LiMn_{1.5}Ni_{0.5}O_4$ [8,9]. We demonstrated that this spinel undergoes a transition metal order ($P4_332$) → disorder ($Fd3m$) transition between 700 and 730 °C in air, which is in close proximity of onset temperature of oxygen loss. Although ordered and disordered states of spinel $LiMn_{1.5}M_{0.5}O_4$ were mentioned in a number of papers [10,11], the underlying reason behind the origin of this transition remains unidentified.

Dahn and co-workers showed the possibility of synthesizing ordered $LiMn_{1.5}M_{0.5}O_4$ at 800 °C in oxygen, whereas disordered spinel was found to form in air atmosphere at same temperature. However, the origin of the phase transformation still remained in question [7]. In another study, the same group and others demonstrated the impact of oxygen-partial-pressure and composition on disproportionation temperature (also onset temperature for oxygen loss, $T_o$) in the 4 V $LiMn_2O_4$ system at high temperature [12–14].

* Corresponding author. Tel.: +1 732 932 6850x608; fax: +1 732 932 6855.
*E-mail address:* muharrem@eden.rutgers.edu (M. Kunduraci).

0378-7753/$ – see front matter © 2007 Elsevier B.V. All rights reserved.
doi:10.1016/j.jpowsour.2006.11.051

To our knowledge, there is no such study in literature that has reported the effect of oxygen-partial-pressure and nickel content on cation ordering in $LiMn_{2-x}Ni_xO_4$. In this study, we synthesized $LiMn_{2-x}Ni_xO_4$ with varying nickel content ($x = 0.36$–$0.50$) in air and compared the structures before and after post-annealing in oxygen and nitrogen atmospheres. The compositions with $x < 0.50$, which contain increasing $Mn^{3+}$ content with decrease in $Ni^{2+}$, were chosen to understand the influence of $Mn^{3+}$ on the destabilization of the transition metal sublattice ordering. Finally, the observations are correlated with the rate capability of spinel to complement the link between cation ordering, $Mn^{3+}$ content and power density of the spinel as a cathode in lithium batteries.

## 2. Experimental

Spinel powders were synthesized as described in more detail elsewhere [8]. Briefly, stoichiometric amounts of metal nitrates were first dissolved in distilled water and added dropwise to ethylene glycol–citric acid solution preheated to 90 °C. After all the nitrate solution was consumed, the solution was kept at this temperature for 30 min for the completion of chelation. After this point, the dark and viscous solution was cast on a stainless steel plate preheated to 140 °C. After residing at this temperature for some time, the solution turned into a thin, porous, dark film due to polymerization of glycol with acid and evaporation of excess water. The final product was ignited in open air and heated to 700 °C in air for 10 h in an alumina crucible to obtain spinel powders. Heating rate was 10 °C $min^{-1}$.

X-ray powder diffraction was taken using a Scintag Inc.X2, diffractometer. The samples were scanned between 15° and 90° at a rate of 0.1° $min^{-1}$ using Cu Kα radiation. Silicon powder was used as internal standard for lattice constant calculations. A Thermonicolet Avatar 360 was used for Fourier transformed infrared study. The spectra of samples were obtained by diluting minute amount of spinel powder in about 100 mg of infrared grade potassium bromide. The spectrum was averaged by 100 scans taken between 4000 and 400 $cm^{-1}$. The resolution was chosen to be 4 $cm^{-1}$. A Hi-Res 2950 Thermogravimetric analyzer was used for thermal analysis.

Two thousand and twenty-five type coin cells were used for electrochemical characterization of spinel powders. The cell consisted of $LiMn_{2-x}Ni_xO_4$ as positive electrode, Li metal as negative electrode and 1 M $LiPF_6$ dissolved in EC-DMC as electrolyte. The positive electrode was fabricated by the Bellcore process composed of 52 wt.% active material, 13 wt.% Super P carbon black and 35 wt.% PVDF-HFP binder dispersed in dibutyl phthalate plasticizer. The reason for low active material loading will be addressed in the text. The slurry was cast and dried in a <2% RH dry room at room temperature. Afterwards, the plasticizer was extracted in ether. The electrode was subjected to final drying at 120 °C under vacuum for overnight. The cell was assembled in a He-filled glovebox and cycled using a Maccor galvanostat cycler.

## 3. Results

We have previously utilized FTIR spectroscopy to differentiate the transition metal ordered $P4_332$ spinels from the disordered spinels of the $Fd3m$ space group. The ordered phase revealed a distinct intensity increase and narrowing along with a space group defining growth of the Ni–O band at 588 $cm^{-1}$. The infrared spectra of spinels used in this study are given in Fig. 1(a and b) for spinels annealed at 700 °C in air and those subsequently annealed in oxygen at 700 °C. For $x \leq 0.42$ in $LiMn_{2-x}Ni_xO_4$, spinels heat-treated in air have been assigned to $Fd3m$ space group. Surprisingly, for $x = 0.44$ we observed a very significant sharpening in its spectrum, implying the existence of cation ordering in this composition. As shown in Fig. 1(b), after oxygen annealing, all compositions developed some degree of transition metal ordering whose magnitude increased with higher Ni content.

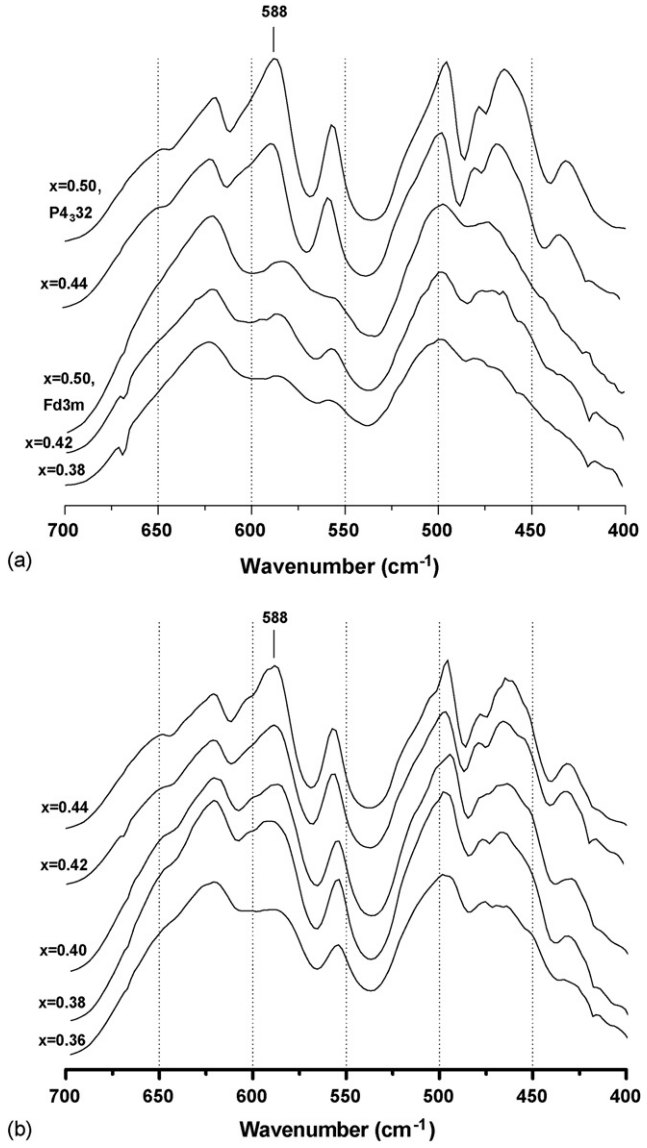


Fig. 1. Infrared spectra of $LiMn_{2-x}Ni_xO_4$: (a) annealed at 700 °C in air, except for $x = 0.50$ $Fd3m$, which was heat-treated at 730 °C for 1 h in air and (b) annealed at 700 °C in oxygen.

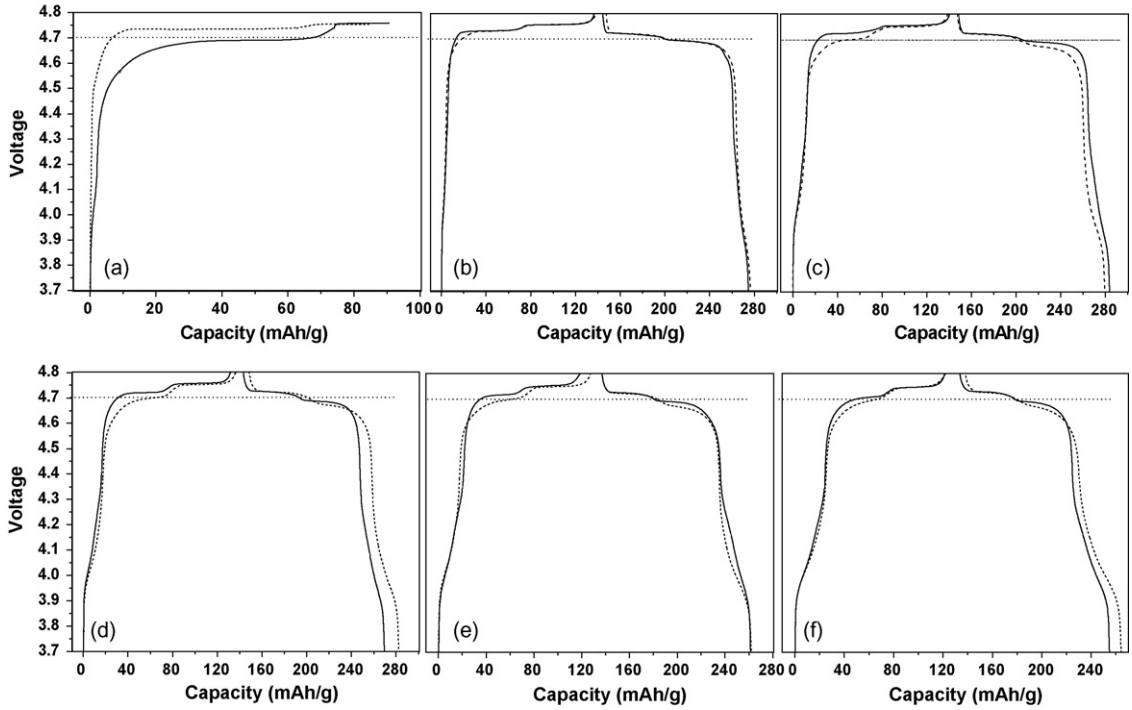


Fig. 2. Charge/discharge voltage profiles of $LiMn_{2-x}Ni_xO_4$ annealed at 700 °C in air (dashed) or oxygen (solid) with the exception that solid line in (a) represent *Fd*3*m* $x = 0.50$ annealed in air at 730 °C for 1 h. (a) $x = 0.50$; (b) $x = 0.44$; (c) $x = 0.42$; (d) $x = 0.40$; (e) $x = 0.38$; (f) $x = 0.36$. The dot line shows the 4.70 V to guide eye.

The charging voltage profile of $LiMn_{1.5}Ni_{0.5}O_4$ can be divided into two regimes: first half was associated with the $Ni^{2+} \rightarrow Ni^{3+}$ transition and the latter was attributed to the $Ni^{3+} \rightarrow Ni^{4+}$ transition [15]. We have identified that the first $Ni^{2+} \rightarrow Ni^{3+}$ "plateau" lies just below 4.70 V (typically ~4.69 V) for the disordered *Fd*3*m* and just above 4.7 V (typically ~4.72 V) for the ordered $P4_332$ spinels (Fig. 2(a)) (this holds only for mid to slow charging rates such as 44 mA $g^{-1}$ used in this study). This result has been found to be reproducible and consistent with another study [8]. This phenomenon can be based on the differing lithium-ion insertion energies into ordered and disordered phases. Keeping this in mind, it is suggested that for a spinel with a mixture of $P4_332$ and *Fd*3*m* phases this regime should be stretched between these two end points, thereby looking like a continuous curve. Then, the amount of capacity below and above 4.70 V line would be commensurate with relative ratios of both phases.

In this regard, the charge/discharge voltage profiles of spinels at third cycle were compared for before and after oxygen annealing and presented in Fig. 2(b–f). The overpotentials (electronic and ionic) that would lead to possible misinterpretation in diagnosis of ordering were minimized using low loading density (~3 mg $cm^{-2}$) electrodes consisting of high wt.% conductive agent (13 wt.% Super P) and nano-size cathode materials. In agreement with infrared study, air annealed samples are cation disordered with the exception for $x = 0.44$ and 0.50. After oxygen annealing, the first regime in spinels for $x \leq 0.42$ shifts above 4.70 V line, substantiating the formation of cation ordering in these spinels. The change although distinct, is less noticeable in cases of $x = 0.36$ and 0.38. This lesser change for the low Ni content materials is entirely consistent with the degree of ordering identified by the intensity development of the key peaks in FTIR.

Besides the increase in voltage for the high voltage plateau, we noticed another change in voltage profile that occurred between 3.9 and 4.3 V that is attributed to $Mn^{4+} \rightarrow Mn^{3+}$ reduction. This regime, which used to be a continuous curve with no features in disordered spinel, developed the appearance of two reaction "plateaus" (Fig. 3). This change is identical to what we have observed in our earlier study when $LiMn_{1.5}Ni_{0.5}O_4$ was

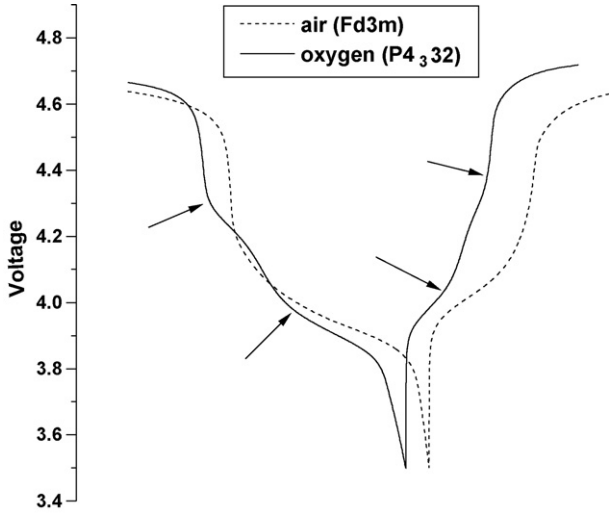


Fig. 3. A segment of the charge/discharge voltage profiles of $LiMn_{1.58}Ni_{0.42}O_4$ spinels annealed at 700 °C in air (*Fd*3*m*) and oxygen ($P4_332$).

Table 1
Summary of electrochemical analysis of $LiMn_{2-x}Ni_xO_4$ before and after oxygen annealing

| $x$ | Capacity around 4 V/overall capacity | | Maximum discharge capacity | | Estimated cation distribution after oxygen annealing |
|---|---|---|---|---|---|
| | Air | Oxygen | Air | Oxygen | |
| 0.44 | 0.107–0.112 | 0.11 | 133.1 | 133.4 | $LiMn_{1.44}^{4+}Mn_{0.12}^{3+}Ni_{0.44}^{2+}O_{4+\delta}$ |
| 0.42 | 0.145–0.15 | 0.145 | 135.5 | 138.7 | $LiMn_{1.438}^{4+}Mn_{0.142}^{3+}Ni_{0.42}^{2+}O_{4+\delta}$ |
| 0.40 | 0.175 | 0.172 | 138.1 | 130.5 | $LiMn_{1.434}^{4+}Mn_{0.166}^{3+}Ni_{0.40}^{2+}O_{4+\delta}$ |
| 0.38 | 0.216 | 0.20–0.203 | 131.5 | 130.7 | $LiMn_{1.428}^{4+}Mn_{0.192}^{3+}Ni_{0.38}^{2+}O_{4+\delta}$ |
| 0.36 | 0.26–0.265 | 0.246–0.25 | 133.1 | 130.9 | $LiMn_{1.403}^{4+}Mn_{0.237}^{3+}Ni_{0.36}^{2+}O_{4+\delta}$ |

Discharge capacity is given in mAh $g^{-1}$.

heated to 850 °C for 2 days and post-annealed at 600 or 700 °C for 3 days (all in air). Similar to the spinels reported here, both spinels contained certain amount of $Mn^{3+}$ population and exhibited an ordered structure. Besides our work, we noticed the very same behavior in Wu and Kim's work [16] (Fig. 3 in their study), but they did not emphasize it. While the origin of this splitting remains unclear now, it seems to be directly related to ordering.

In addition to the voltage shift that was used to explain disorder–order transition upon post-oxygen annealing, other information that is of high importance is the ratio of the 4 V plateau capacity to overall capacity. The former capacity is directly proportional to the concentration of $Mn^{3+}$ present in spinel. Assuming that $Mn^{3+}$ or $Ni^{2+}$ cations are equal in electrochemically activity, the percent capacity in this regime (%4 V) corresponds to $(Mn^{3+})/(Mn^{3+} + 2Ni^{2+})$. The atomic compositions of spinels were estimated by using this capacity and a fixed stoichiometry determined by the nominal compositions are presented in Table 1 with other electrochemical data. It should be noted that that only very small changes in the 4 V plateau (and therefore $Mn^{3+}$ content) exists between the air and oxygen annealed samples. In contrast, larger differences exist between compositions due to their relative differences in $Mn^{3+}$ content brought about by changes in nominal composition, *i.e.* Ni/Mn ratio. Air annealed samples have slightly less %4 V than theoretically expected values. This result possibly stems from the difference in purities of metal nitrate precursors. The data suggest that the chemical composition of the spinel may be slightly deviated from the nominal values. However, this should not affect the argument we brought up in this work since there is a clear trend in structural and electrochemical results induced by post-oxygen-annealing.

The X-ray powder diffraction spectra of spinels for $x = 0.50$, 0.44 and 0.42 before and after oxygen annealing are shown in Fig. 4. We could identify a secondary NiO phase only in $LiMn_{1.5}Ni_{0.5}O_4$, which might be tied with the solubility limit of nickel in this composition as $x$ approaches 0.50. It is interesting to note that same second phase development was observed after anneals in oxygen-poor and -rich atmospheres. It seems that nickel atoms are the first to be ejected from spinel when system is perturbed. Concerning the other samples including those not shown here, there is no noticeable difference between spectra of air and oxygen annealed spinels (high sensitivity 12 h XRD scans were used).

The lattice constants of spinels as a function of composition and annealing atmosphere are plotted in Fig. 5. Regardless of synthesis atmosphere, the lattice constant becomes smaller with

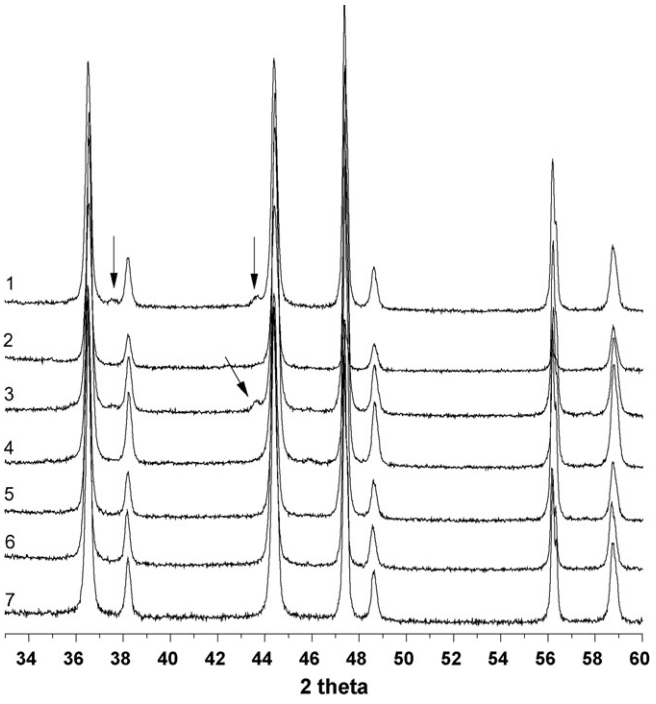


Fig. 4. X-ray powder diffraction spectra of $LiMn_{2-x}Ni_xO_4$ annealed under different atmospheres. All samples were heat treated at 700 °C for 15 h. (1) $x = 0.50$, nitrogen (2) $x = 0.50$, air (3) $x = 0.50$, oxygen (4) $x = 0.44$, air (5) $x = 0.44$, oxygen (6) $x = 0.42$, air (7) $x = 0.42$, oxygen.

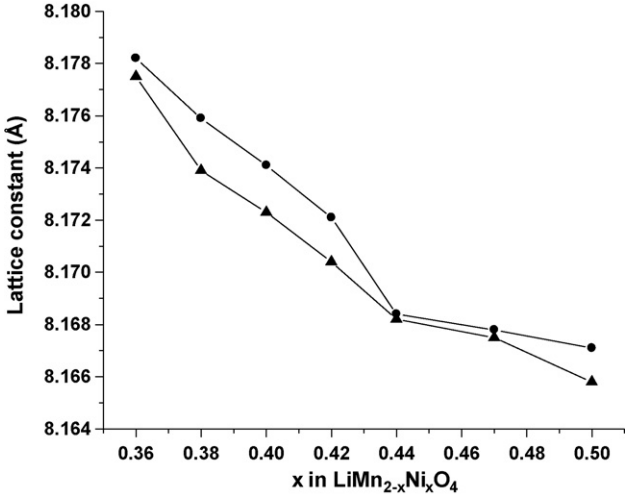


Fig. 5. Lattice constant of $LiMn_{2-x}Ni_xO_4$ with respect to nickel content in spinel. The annealing atmosphere is air for (●) and oxygen for (▲). Annealing temperature is 700 °C for all.

increasing nickel content in spinel. This is an expected trend since charge neutrality necessitates the replacement of larger $Mn^{3+}$ ions by smaller $Mn^{4+}$ ions with increasing nickel content in spinel. Secondly, spinels underwent slight, but noticeable decreases in their lattice constants after oxygen annealing. That holds mostly for $x = 0.42$, 0.40 or 0.38, where disorder–order transition is most significant in terms of its magnitude shown in the aforementioned FTIR results. The reduction in lattice volume was attributed to the $Mn^{3+} \rightarrow Mn^{4+}$ transformation, as evidenced by change in the 4 V plateau, despite being minor in amount.

It was observed that: (i) $Fd3m \rightarrow P4_332$ transition is possible after post-annealing in an oxygen atmosphere and (ii) $LiMn_{2-x}Ni_xO_4$ for $x \geq 0.42$ is $P4_322$ when annealed in air at 700 °C. This indicates that the transition metal ordering of a spinel, at a certain temperature, is dictated by both the annealing atmosphere's oxygen-partial-pressure and the nickel content of the spinel. Regarding the former, experiments showed that the disorder → order transition induced by oxygen annealing could take place in reverse order as well, namely order → disorder transition after post-annealing at lower oxygen-partial-pressure. To demonstrate the sensitivity to both atmosphere and Ni content, we constructed a $pO_2$–T–$x$ diagram (oxygen-partial-pressure; temperature; composition) of this spinel system while focusing on the vicinity of transition temperature $T_c$. The oxygen-partial-pressure in annealing atmosphere ($pO_2$) was studied at three simple discreet values for $pO_2 = 1$ (oxygen), 0.21 (air) and <5 ppm (nitrogen). Spinels that were preheat-treated at 700 °C in air were post-annealed in different atmosphere between 630 and 860 °C for overnight (∼15 h). The data points were collected every 10 °C. After "slow cooling" to room temperature, the infrared spectrum of each spinel was taken to diagnose ordered and disordered phases (overall more than 50 samples were studied). In order to avoid any confusion, the ordered and disordered phases of identical composition (*e.g.* 700 °C air-annealed *Fd3m* and oxygen-annealed $P4_332$ $LiMn_{1.58}Ni_{0.42}O_4$, or 700 °C air-annealed $P4_332$ and 400 °C air-annealed *Fd3m* $LiMn_{1.53}Ni_{0.47}O_4$ for 660 °C nitrogen test) were used occasionally to conclude if the state of spinel prior to experiment has an influence on reaching the equilibrium state. The minor differences between infrared spectra indicated that 15 h was long enough to reach equilibrium regardless of the ordering state existing before the anneal.

Fig. 6 shows the $pO_2$–T–$x$ diagrams of ordered and disordered phases. The diagrams demonstrate the impact of oxygen-partial-pressure on the formation of transition metal ordering. Atmosphere impact is very significant in spinels for $0.47 \geq x \geq 0.40$. In these spinels the highest temperature (we refrained from calling it $T_c$, see Section 4) at which last trace of ordered phase is observed when annealed in oxygen is as much as 150 °C higher in temperature than for anneals done in air. Concerning spinels for $x = 0.36$ and 0.38, even though infrared analysis detected ordered phases at elevated temperatures even in oxygen-rich medium, the percentage of ordering

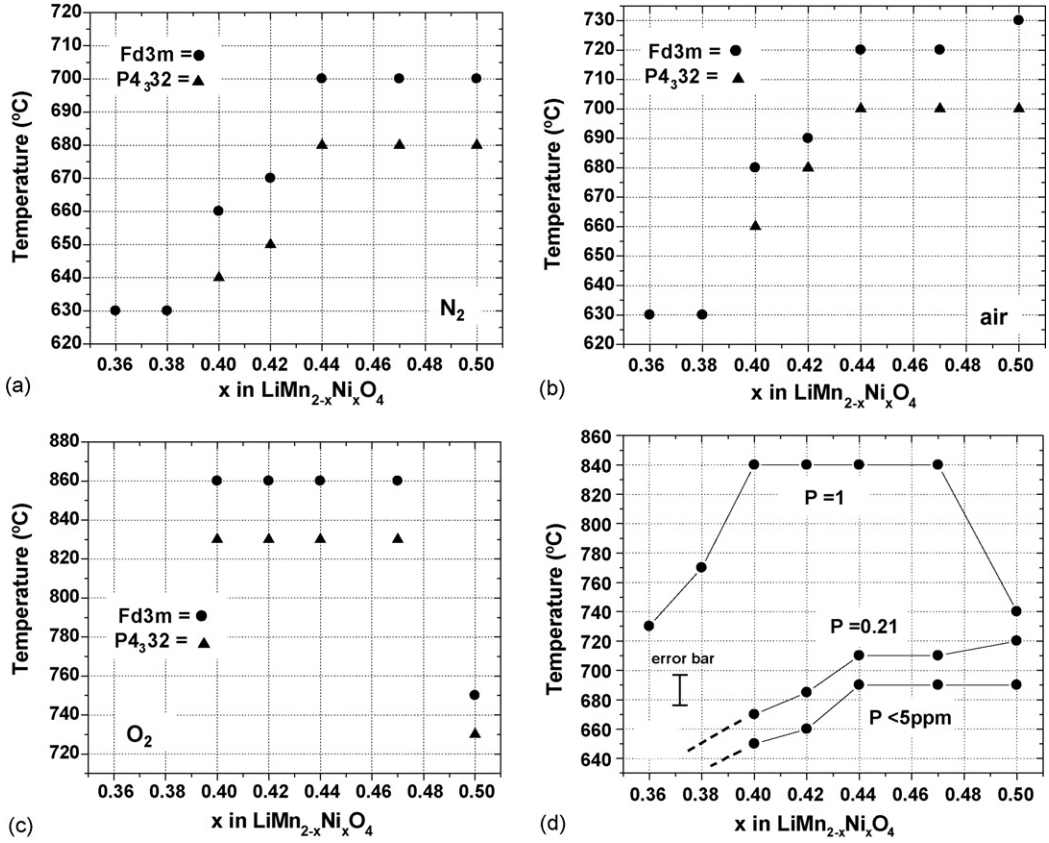


Fig. 6. $T$–$x$ diagram of ordered and disordered phases of spinel $LiMn_{2-x}Ni_xO_4$ under different oxygen-partial-pressures ($pO_2$). (a) $pO_2 < 5$ ppm, nitrogen (b) $pO_2 = 0.21$ ppm, air (c) $pO_2 = 1$ ppm, oxygen. (d) The boundary lines separating fully disordered phases (regimes above the solid line) from partially or fully ordered phases for different annealing mediums.

Table 2
Summary of the structural changes upon post-nitrogen-annealing at different temperatures for $x = 0.42$ and 0.50 in $LiMn_{2-x}Ni_xO_4$

| Heat treatment | Space group | Lattice constant (Å) |
|---|---|---|
| $LiMn_{1.58}Ni_{0.42}O_4$ | | |
| 700 °C-air | *Fd3m* | 8.1722 |
| 700 °C-air + 670 °C-nitrogen | *Fd3m* | 8.1729 |
| 700 °C-air + 650 °C-nitrogen | Partially $P4_332$ | 8.1705 |
| 700 °C-air + 630 °C-nitrogen | Partially $P4_332$ | 8.1705 |
| $LiMn_{1.50}Ni_{0.50}O_4$ | | |
| 700 °C-air | $P4_332$ | 8.1671 |
| 700 °C-air + 700 °C-nitrogen | *Fd3m* | 8.1696 |
| 700 °C-air + 680 °C-nitrogen | $P4_332$ | 8.1667 |
| 700 °C-air + 660 °C-nitrogen | $P4_332$ | 8.1663 |

is very minor. In cases of air and nitrogen annealing, no ordered phase in these spinels was seen down to 630 °C. There is an anomaly with $LiMn_{1.50}Ni_{0.50}O_4$. The maximum temperature to obtain ordered phase is significantly lower than those of other spinels. While this point remains unclear for now, it might be linked with nickel solubility, secondary phase formation or slight non-stoichiometry in initial composition.

It was noted that the lattice volume of spinel decreased even after post-annealing in an oxygen-poor environment as demonstrated with spinel for $x = 0.42$ and 0.50 (Table 2). This is contrary to what one would expect as this environment should induce the formation of large $Mn^{3+}$ cations. It should be noted that a small amount of a secondary phase (NiO) was noticed in the $x = 0.42$ spinel after the heat treatment, which possibly induced a change in the $Mn^{3+}/Mn^{4+}$ ratio in this material and a subsequent change in its lattice parameter. However, when the same spinels were heated to a slightly higher temperature, spinel turned into (for $x = 0.50$) or stayed a (for $x = 0.42$) fully cation disordered *Fd3m* and its lattice volume increased with formation of larger $Mn^{3+}$. This observation together with previously mentioned changes in lattice volume after exposure to oxygen-rich atmosphere indicates that the shrinkage in lattice volume, whether in oxygen-rich or poor atmosphere, may be in part linked with creation of ordering along with Mn oxidation state.

## 4. Discussion

In this part, we will try to answer the open question; what is the basis of the oxygen-partial-pressure and the nickel content dependence of cation ordering?

Earlier we have reported that the $T_c$ of $LiMn_{1.5}Ni_{0.5}O_4$ coincided with the onset temperature of oxygen loss from ordered spinel ($T_o$, ~715 °C). Because of the oxygen loss, a portion of $Mn^{4+}$ was reduced to $Mn^{3+}$ during the transformation of ordered spinel into a disordered state. The mechanism is illustrated below:

$$LiMn_{1.5}{}^{4+}Ni_{0.5}{}^{2+}O_4(P4_332) \Leftrightarrow Li_{1-A}Mn^{4+}Mn^{3+}Ni_{0.5-B}{}^{2+}O_{4-\delta}(Fd3m) + Li_ANi_BO + O_{2(g)}$$

A question remains to whether the ordering is destroyed above $T_c$ due to oxygen loss, introduction of $Mn^{3+}$, deviation from 3:1 transition metal ratio (off-stoichiometry) or it is just a thermally induced phase transition. After the results presented here, we know now conclusively that $Mn^{3+}$ and off-stoichiometry are to be excluded from the discussion as spinels with significant $Mn^{3+}$ population, such as $LiMn_{1.56}Ni_{0.44}O_4$ in which 7–8% of manganese ions are existent as $Mn^{3+}$, can indeed form the ordered structure. It is also possible to speculate that the spinel is segregated into a composite where the $Mn^{4+}$ rich domains form a $P4_332$ ordered spinel and the $Mn^{3+}$ domains form a disordered *Fd3m*. However, the electrochemical data does not support this. The first plateau in $LiMn_{1.56}Ni_{0.44}O_4$, which is considered to be ordered $P4_332$, is uniform and occurs above 4.70 V, indicating the absence of mixed phases. If indeed there were segregated phases we would expect to see a percentage of the voltage profile below 4.70 V commensurate with the percentage of the *Fd3m* phase.

In an effort to correlate $T_c$ with $T_o$, we have performed thermogravimetric analyses on different spinels under air, oxygen and nitrogen. The derivative of %weight *versus* temperature curve ($-dM/dT$ *versus* $T$) plots of spinels for $x = 0.44$ and 0.50 are shown in Fig. 7(a and b) (heating rate: 5 °C min$^{-1}$). The apex of the most intense peak exhibited an expected variation with oxygen-partial-pressure but minor change with nickel content, namely around 650, 730 and 750 °C under nitrogen, air and oxygen, respectively. However, these numbers are to be treated as a relative trend as we noticed significant shifts in these temperatures when heating rate was changed to 2 °C min$^{-1}$ (−16 °C) and 10 °C min$^{-1}$ (+27 °C). The effect of heating rate was minor in the last two environments (3–5 °C).

TGA revealed a trend in profile that clearly distinguished ordered phase from disordered one. As opposed to a sharp transition of weight loss in ordered phases, $-dM/dT$ *versus* $T$ profiles of disordered phases lacked such a sharp peak. This distinction is much clearer when profiles of ordered and disordered phases of same spinel on either side of transition temperature are compared (certain samples in Fig. 7(b and c)). In an effort to identify this sharp peak we stopped the TGA run at three different points (see Fig. 7(d)) and took their infrared spectrum after "fast cooling" to room temperature. The spinels had ordered phase only at the data point just before the start of sharp peak, thereby indicating that this intense peak should be linked with order–disorder transformation. We used the relative ratios of two peaks in TGA profiles as a means of assessing percentage of ordering in spinels (similar to our approach in infrared spectroscopy) and as another tool in construction of diagram.

That the ordered spinel transformed into a cation disordered structure after fast cooling from approximately 730 °C in oxygen-rich atmosphere contradicts with the diagram in Fig. 6(c). In addition, quenching spinels from high temperatures (*e.g.* 800 °C) during oxygen annealing revealed disordered *Fd3m* phase. We suggest that it is the oxygen uptake during slow cooling that induces a fully or partially ordered phase after annealing to high temperatures in oxygen atmosphere. Therefore, the real $T_c$ lies around 720 ± 10 °C for $pO_2 = 0.21$ and 1, and 650 ± 20 °C for nitrogen atmosphere, which are

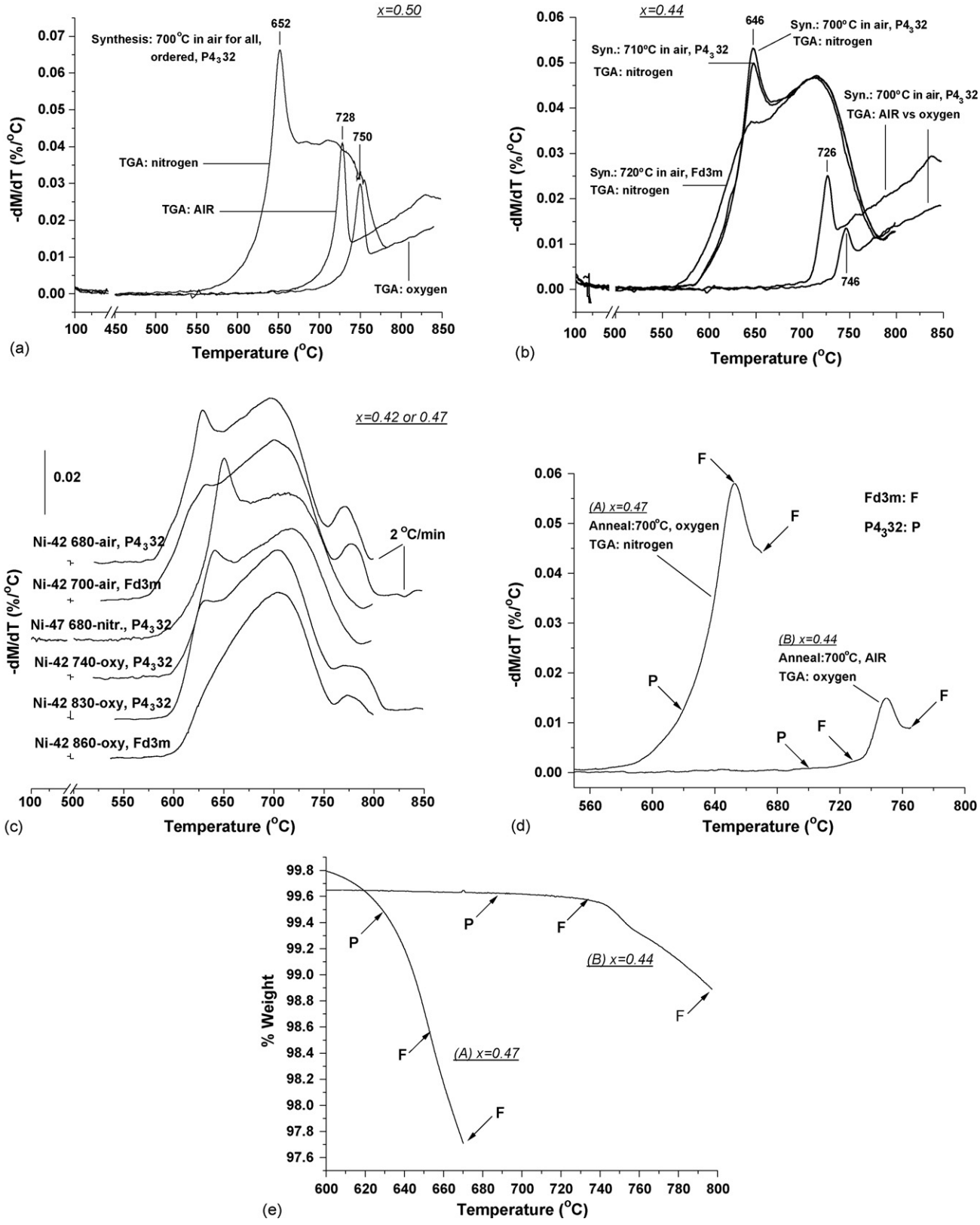


Fig. 7. The $-dM/dT$ *vs. T* curves of ordered and disordered phases $LiMn_{2-x}Ni_xO_4$ spinels for different anneals (temperature and annealing medium) and TG analyses. (a) $x = 0.50$; (b) $x = 0.44$; (c) $x = 0.42$ or 0.47; (d) $x = 0.47$ or 0.44. Heating rate in TGA is 5 °C $min^{-1}$ unless told otherwise. In (c), TGA atmosphere is nitrogen for all and profiles were shifted up for clarity. (e) %Weight *vs. T* curves of spinels in (d).

in proximity of $T_o$'s of the corresponding atmospheres. On the other hand, due to large inaccuracy in determination of onset temperature, our argument about the dependence of $T_0$ on oxygen-partial-pressure remains open for discussion at this moment. As a final note, just prior to the submission of this paper, Sato and co-workers reported on post-oxygen annealing in $LiNi_{0.5-x}Co_{2x}Mn_{1.5-x}O_4$ [17]. In their study, spinels for $2x = 0.05$ ($T_0 > 700\,^\circ C$) and 0.10 ($T_0 < 700\,^\circ C$) were ordered $P4_332$ and disordered $Fd3m$, respectively, when annealed at 700 °C in air.

With respect to the role of nickel content, as the spinel composition deviates more and more from $LiMn_{1.5+x}Ni_{0.5-x}O_4$ (higher $x$), the $Mn^{3+}$ concentration in spinel will increase. In many studies in literature, ionic size mismatch and charge difference between crystallographic lattice points (4b and 12d in our case) has been named as a driving force in creation of ordering in different oxide systems [18]. If we assume that $Mn^{3+}$ population is split over these two lattice points in ordered spinels, increasing $Mn^{3+}$ concentration would reduce the average size and charge differences between 4b and 12d sites and this would in return diminish the driving force to form ordered structures ($Mn^{3+}$: 65 pm, $Ni^{2+}$: 69 pm, $Mn^{4+}$: 54 pm). In the light of this proposition, we can expect to see a smaller stability window for spinels with less nickel content, *i.e.* smaller $T_c$.

Regarding the possibility of splitting of $Mn^{3+}$ over two crystallographic sites in ordered systems, we searched literature for ternary ordered spinels where octahedral positions are occupied by three different ions. Wolska et al. studied $Li_{0.5}Fe_{2.5}O_4/LiMn_2O_4$ solid solution and reported that within certain composition range spinel forms ordered structure [19]. According to their Rietveld analysis, $Li^+$, $Fe^{3+}$, $Mn^{3+}$ and $Mn^{4+}$ ions populate the 4b and 12d sites in this structure randomly. Similarly, Scharner et al. reported on cation distribution in ordered spinels of $Li_2O$–$Fe_2O_3$–$TiO_2$ system [20]. According to their results, $Li^+$, $Fe^{3+}$ and $Ti^{4+}$ ions occupy 12d sites in ordered spinels while 4b sites are exclusively inundated with $Li^+$. In light of these studies, our conclusion to support ordering for $Mn^{3+}$ containing spinels is plausible.

Earlier we have reported that the intrinsically poor electronic conductor $P4_332$ $LiMn_{1.5}Ni_{0.5}O_4$ was outperformed by better electronic conductor $Fd3m$ $LiMn_{1.5}Ni_{0.5}O_{4-\delta}$ when discharged at high rates. It is controversial at this point whether electronic conductivity, derived by the presence of $Mn^{3+}$, or the electrochemically induced loss of ordering, as suggested elsewhere [10], is the basis of this distinction. We demonstrated the feasibility of high rate capabilities with ordered spinel by using enough conductive agent (external) in electrode formulation. In this respect, it is believed that the comparison of rate capabilities of spinels before and after oxygen annealing would be a very intriguing task since this would totally eliminate the role of electronic conductivity as both phases have the same intrinsic (similar $Mn^{3+}$ content) and extrinsic (same amount of conductive agent) electronic conductivities. This electrochemical study was limited to $x \geq 0.40$ in $LiMn_{2-x}Ni_xO_4$. The spinels for $x = 0.38$ and 0.36 have been excluded since their voltage profiles (even after oxygen annealing) show poor resemblance to that of an ordered 4.7 V spinel with zero 4 V plateau (single phase *versus* two-phase progression during the first half of charging for the former and the latter, respectively). This characteristic is relatively negligible in cases of $x = 0.40$ and 0.42. The electrochemical results are summarized in Fig. 8. The discharge current densities were selected as 700, 1500 and 2500 mA $g^{-1}$. The relative percent capacities are with respect to those when discharged at 44 mA $g^{-1}$. As is seen clearly, there is no degradation in rate capabilities after transformation to ordered state, or oxygen annealing. The best performance rate performance was isolated for high $Mn^{3+}$ content spinels consistent with our previous electronic conductivity studies. This is supportive to our argument brought up earlier. However, the rate story will be sealed only when the power densities of ordered and disordered spinels (with and without $Mn^{3+}$) are compared using powders with coarser particle sizes, which is currently in progress. This is based on the possibility that the ordering process may affect the intrinsic lithium diffusion and these effects will be exasperated only with spinels of larger particle size.

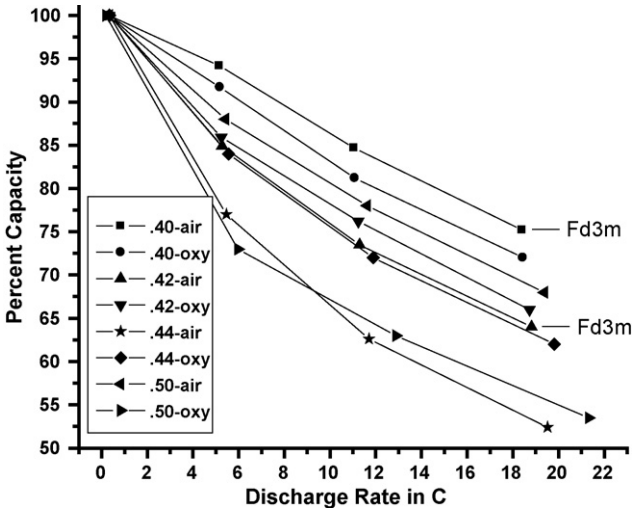


Fig. 8. Rate capability of $LiMn_{2-x}Ni_xO_4$ ($0.50 \geq x \geq 0.40$) for anneals in air and oxygen. $1C = 1$ h discharge. Cells were discharged at room temperature.

## 5. Conclusion

The nickel content in $LiMn_{2-x}Ni_xO_4$ and oxygen-partial-pressure in the annealing atmosphere have been demonstrated to influence the transition metal order–disorder transition temperature significantly. This phase transition was suggested to result from oxygen loss from ordered spinel as opposed to the presence of $Mn^{3+}$ thereby suggesting an influence of the oxygen sublattice on the transition. The underlying reason behind the observed dependence of the order–disorder transition temperature on oxygen-partial-pressure was linked with oxygen loss from spinel. In other words, the disorder–order transition corresponds to the onset temperature of oxygen loss from spinel. The spinels tend to form ordered structure with increasing nickel content. This phenomena was consistent with a steric component to the $Ni^{2+}/Mn^{4+}$ ordering, which is perturbed by the presence of the $Mn^{3+}$ cation for highly off-stoichiometric compositions.

The rate capability of nano-structured $LiMn_{2-x}Ni_xO_4$ spinels was not correlated to transition metal order or disorder, but only the presence of $Mn^{3+}$.

## Acknowledgements

The authors like to thank The US Government for financial support.

## References

[1] H.C. Shin, W.I. Cho, H. Jang, J. Power Sources 159 (2006) 1383.
[2] M. Takahashi, S. Tobishima, K. Takei, Y. Sakurai, Solid State Ionics 148 (2002) 283.
[3] A.K. Padhi, K.S. Nanjundaswamy, J.B. Goodenough, J. Electrochem. Soc. 144 (1997) 1188.
[4] K. Ariyoshi, S. Yamamoto, T. Ohzuku, J. Power Sources 119–121 (2003) 959.
[5] T. Ohzuku, S. Takeda, M. Iwanaga, J. Power Sources 81–82 (1999) 90.
[6] Y. Sun, Z. Wang, X. Huang, L. Chen, J. Power Sources 132 (2004) 161.
[7] Q. Zhong, A. Bonakdarpour, M. Zhang, Y. Gao, J.R. Dahn, J. Electrochem. Soc. 144 (1997) 205.
[8] M. Kunduraci, G.G. Amatucci, J. Electrochem. Soc. 153 (2006) A1345.
[9] M. Kunduraci, J.F. Al-Sharab, G.G. Amatucci, Chem. Mater. 18 (2006) 3585.
[10] J.H. Kim, S.T. Myung, C.S. Yoon, S.G. Kang, Y.K. Sun, Chem. Mater. 16 (2004) 906.
[11] Y. Idemoto, H. Narai, N. Koura, J. Power Sources 119–121 (2003) 125.
[12] Y. Gao, J.R. Dahn, J. Electrochem. Soc. 143 (1996) 1783.
[13] J.M. Paulsen, J.R. Dahn, Chem. Mater. 11 (1999) 3065.
[14] J.M. Tarascon, W.R. McKinnon, F. Coowar, T.N. Bowmer, G.G. Amatucci, D. Guyomard, J. Electrochem. Soc. 141 (1994) 1421.
[15] Y. Terada, K. Yasaka, F. Nishikawa, T. Konishi, M. Yoshio, I. Nakai, J. Solid State Chem. 156 (2001) 286.
[16] X. Wu, S.B. Kim, J. Power Sources 109 (2002) 53.
[17] D. Li, A. Ito, K. Kobayakawa, H. Noguchi, Y. Sato, J. Power Sources 161 (2006) 1241.
[18] W. Branford, M.A. Green, D.A. Neumann, Chem. Mater. 14 (2002) 1649.
[19] E. Wolska, P. Piszora, K. Stempin, C.R.A. Catlow, J Alloys Compd. 286 (1999) 203.
[20] S. Scharner, W. Weppner, P. Schmid-Beurmann, J. Solid State Chem. 134 (1997) 170.